Radioprotection 1995
Vol. 30, n° 4, pages 509 à 518

Article

Neutron flux imaging with nuclear track detectors

A. SEGHOUR*, **, S. DJEFFAL*, J.C. SENS**, A. STAMPFLER**

(Manuscrit reçu le 9 décembre 1994, révisé le 24 février 1995, accepté le 4 avril 1995)

RÉSUMÉ **Les résultats d'une investigation des variations du flux de neutrons d'un site d'irradiation aux neutrons thermiques à l'aide de matériaux convertisseurs neutron-particules chargées et de détecteurs solides de traces nucléaires (DSTN) sont reportés. Dans ce contexte, trois cartes de faisceaux de neutrons ont été établies et analysées. Les cartographies de neutrons obtenues en utilisant le convertisseur BN1, qui a été trouvé plus sensible aux variations de neutrons que le tétraborate de lithium, ont permis la localisation des zones de concentration neutronique. Les résultats des mesures du flux moyen de neutrons, obtenus à l'aide de la technique des DSTN, sont en bon accord avec ceux obtenus par la technique conventionnelle de mesure de flux par activation neutronique de feuilles.**

ABSTRACT **The results of an investigation on the spatial variations of neutron flux using neutron-charged particle converter materials and solid state nuclear track detectors in a thermal neutron irradiation site are reported. In this context, three neutron beam maps have been established and analyzed. Neutron flux cartographies performed with the BN1 converter, which has been found to be more sensitive to neutron flux variations than the lithium tetraborate converter, have allowed location of neutron concentration areas. The results of average neutron flux measurements obtained by means of the SSNTD technique are in good agreement with those obtained using the conventional technique of neutron flux measurement by activation of foils.**

1. Introduction

Solide state nuclear track detectors (SSNTD) have been used to perform neutron induced autoradiography in fields such as biology [2, 5] medicine [1, 7] and solid state science and technology [9]. This is possible by detection of the charged particles produced by neutron induced nuclear reactions in the sample itself (autoradiography) or in a converter placed between the sample and the detector (neutron imaging). Converter materials with high B or Li concentra-

* Laboratoire de dosimétrie, Centre de radioprotection et de sûreté, 02 boulevard Frantz Fanon, BP 1017, 16000 Alger, Algeria.
** Service du réacteur nucléaire universitaire, Centre de recherches nucléaires et Université Louis Pasteur, 23 rue du Loess, 67037 Strasbourg Cedex 2.

tions are generally used under thermal neutron irradiations. For fast neutrons, the converter material consists simply of a thin polyethylene sheet which enhances neutron-recoil proton conversion.

Neutron flux measurements are usually performed by means of neutron activation of Au, Cu or Co foils. The size of the foils should be chosen small enough to avoid flux depression and self-shielding phenomena which can perturb flux measurement and induce errors on thermal neutron flux evaluation [4]. Small foils are also more suitable for gamma spectroscopy and for counting. For this reason, neutron flux imaging of large areas may be performed using a set of small circular foils distributed over the concerned area. Nevertheless, the isoflux levels are dependent on the number of foils which must be important for a precise neutron flux cartography. Unfortunately, for an important set of foils and in addition to the problem of positionning, the interchange and mixing of foils become more and more probable, which may lead to a result in non-accordance with the real spatial distribution of the neutron flux at the position of interest.

SSNTDs, which may be obtained in large size, combined with an appropriate neutron-charged particles converter, can register neutron flux variations with a few millimeters steps. As it will be seen below, the entire SSNTD sheet exposed with its converter to a neutron flux gives a faithful image of the spatial distribution of the incident neutron flux at the measurement site.

In this work, large sheets (10 x 10 cm^2) of SSNTD pressed against converter materials, *i.e.* lithium tetraborate $Li_2B_4O_7(5H_2O)$ and BN1 (Dosirad, Kodak Pathé France), have made it possible to investigate the spatial variations of neutron flux in a thermal column of the Strasbourg University nuclear reactor (SUNR).

2. Experimental procedure

The detection assembly at the irradiation position of the vertical thermal canal VC3 of the SUNR is shown in Figure 1. CR-39 foil, 250 μm thick, provided by Pershore Mouldings (U.K.) was pressed against converter materials $Li_2B_4O_7(5H_2O)$ and BN1. This assembly was centered at the upper end of VC3. It had been previously established by neutron spectroscopy measurements with surface barrier detectors and a ^6LiF target that neutrons at this irradiation position were completely thermalized [6]. Unidirectionality of the delivered beam was guaranteed by a 1 m high cylindrical Cd tube in contact with the inner wall of the canal, which eliminates neutrons with trajectories not parallel to the canal axis by (n, γ) reactions.

The attenuation of the neutron flux after crossing the cellulose nitrate CN85 when using a $Li_2B_4O_7(5H_2O)$ converter and a polyester support of BN1 is negligible. After irradiation, CR-39 was chemically etched in 20% NaOH solution at 60°C during 2 h.

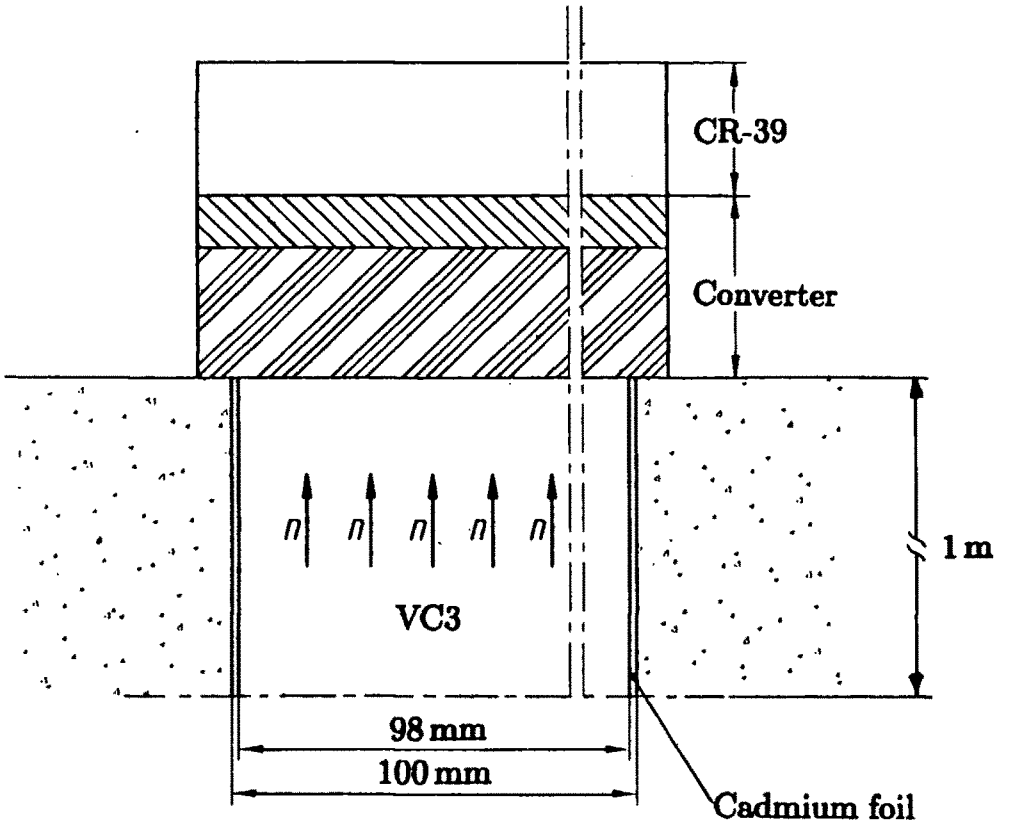

Fig. 1 – Detection assembly at the irradiation position of thermal column VC3. Converters used are $Li_2B_4O_7(5H_2O)$ and BN1.
Dispositif expérimental de détection à la sortie du canal thermique VC3. Les convertisseurs utilisés sont $Li_2B_4O_7(5H_2O)$ et BN1.

Two track counting modes have been used : automatic and optical. Tracks of particles produced in the $Li_2B_4O_7(5H_2O)$ converter were counted using an image analyser system. An effective detection area of ~ 42 cm^2 was divided into 6 sectors of 2 x 3.5 cm^2. Each sector was systematically scanned at 28 unitary field of 75 x 50 μm^2 area by means of automatic lateral and longitudinal displacements with 0.5 cm step. Optical counting was used for the BN1 converter where the entire detector surface area was scanned with 2 mm step displacements to obtain more information about the flux variations.

3. Results and discussion

Because of their low energy, thermal neutrons can only produce tracks in CR-39 detectors by means of nuclear reactions in an external neutron-charged particle converter. The ^{10}B and ^{6}Li isotopes (with respective natural abundances of 20% and 7%) present high (n, α) cross sections for thermal neutrons (3 837 and 940 barns respectively) so that converters with low concentration of B and Li can yield an appreciable response in CR-39 detectors.

Only charged particles produced at distances from the surface of the detector smaller than their ranges in the converter medium can reach the detector and produce etchable tracks.

The range r of charged particles in a composite medium of density d and mean atomic number A is given by the approximate Bragg-Kleeman formula [3] :

$$r = r_0 \left(\frac{d_0}{d} \right) \left(\frac{A}{A_0} \right)^{1/2} \quad (1)$$

where r_0, d_0 and A_0 are the range, density and mean atomic number of the reference medium (water) respectively.

The mean atomic number is defined as [8] :

$$A = \frac{\sum_i n_i A_i}{\sum_i n_i} \quad (2)$$

with :

n_i : number of atoms (i) in the molecular compound,

A_i : atomic number of the atom (i).

Ranges of the produced particles, calculated according to equation (1), are reported in Table I for the two converters used $Li_2B_4O_7(5H_2O)$ and BN1.

TABLE I

Calculated ranges of the particles produced in lithium tetraborate and BN1 converters
Parcours calculés des particules produites dans les convertisseurs au tétraborate de lithium et au BN1 et conditions d'irradiation

Reaction	Produced particle	Energy (MeV)	Range in water (µm)	Range in $Li_2B_4O_7(5H_2O)$ (µm)	Range in BN1 (µm)
$^{10}B(n, \alpha)^7Li$	α (6%)	1.78	8.9	22.10	12.58
	^7Li (6%)	1.01	4.5	11.18	6.36
	α (94%)	1.47	7.2	17.88	10.17
	$^7Li^*$ (94%)	0.84	4.0	9.94	5.65
^6Li (n, t)α	t	2.73	60.4	150.02	
	α	2.05	10.5	25.83	

* ^7Li is produced in an excited level which decays to the ground state by γ emission of 0.48 MeV.

Charged particles from thermal neutron induced reactions $^{10}B(n, \alpha)^{7}Li$ and $^{6}Li(n, t)\alpha$ are emitted isotropically over a 4π solid angle. Only those particles emitted from the infinitesimal volume $dV = ds \times dx$ within an angle ranging between $\theta = 0°$ and $\theta = \theta_c$ as shown in Figure 2 can produce etchable tracks in CR-39. Under etching conditions given above, the bulk etch velocity V_B has been found to be approximately 0.4 µm h^{-1} so that the removed detector thickness is $\simeq$ 0.8 µm during the etching time.

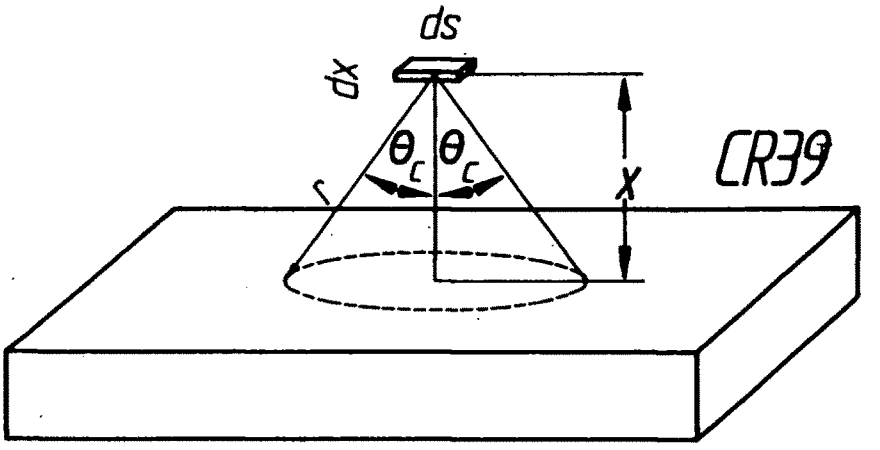

Fig. 2 – Critical emission angle θ_c for etchable tracks.
Angle critique d'émission θ_c pour les traces révélables.

The critical emission angle θ_c is then given by :

$$\cos \theta_c = \frac{x}{r} \tag{3}$$

where x is the distance from the reaction site to the detector surface and r the range of the emitted particle in the converter material.

The ratio ρ of the detected particle to the total emitted particles is given by the geometric factor :

$$\rho = \int_0^{2\pi} \int_0^{\theta_c} d\phi \, \sin\theta \, d\theta \, / \int_0^{2\pi} \int_0^{\pi} d\phi \, \sin\theta \, d\theta = \frac{1 - \cos\theta_c}{2} \tag{4}$$

The number of tracks recorded in CR-39 and originating from the volume dV is :

$$\frac{dN}{dV} = \frac{1}{2}\left[\left(0.06\,(\rho_1 + \rho_2) + 0.94\,(\rho_3 + \rho_4)\right) N_B \sigma_B + P(\rho_5 + \rho_6) N_{Li} \sigma_{Li}\right] \Phi t \tag{5}$$

where :

ρ_1, ρ_2, ρ_3 and ρ_4 are the geometrical factors of the charges particles emitted by the $^{10}B(n, \alpha)^{7}Li$ reaction, whereas ρ_5 and ρ_6 correspond to the reaction $^{6}Li(n, t)\alpha$ (Table I),

Φ : neutron flux ($cm^{-2}\ s^{-1}$),

t : irradiation time (s),

N_B, N_{Li} : number of ^{10}B and ^{6}Li atoms per unit volume (cm^{-3}),

σ_B, σ_{Li} : neutron crosse section of $^{10}B(n, \alpha)^{7}Li$ and $^{6}Li(n, t)\alpha$ in cm^2,

and :

$$P = \begin{cases} 1 & \text{for the } Li_2B_4O_7(5H_2O) \text{ converter.} \\ 0 & \text{for the BN1 converter.} \end{cases} \tag{6}$$

The factor (1/2) expresses the fact that in thermal neutron induced reactions, two particles are emitted in opposite directions. Only one particle per reaction reaches the detector.

In order to obtain the number of recorded tracks per unit area (dN/dS), one has to integrate (dN/dV) over values of x between $x = 0$ (contact CR-39) to $x = r_i$ for each particle. So we get :

$$\frac{dN}{dS} = \frac{1}{2}\left[\left(0.06\left(\int_0^{r_1}\rho_1\,dx + \int_0^{r_2}\rho_2\,dx\right) + 0.94\left(\int_0^{r_3}\rho_3\,dx + \int_0^{r_4}\rho_4\,dx\right)\right)N_B\sigma_B + P\left(\int_0^{r_5}\rho_5\,dx + \int_0^{r_6}\rho_6\,dx\right)N_{Li}\sigma_{Li}\right]\Phi t \tag{7}$$

Combining equations (4) and (7) one obtains for the $Li_2B_4O_7(5H_2O)$ converter (d = 0.5 g cm^{-3}, mass fractions : Li = 5.36%, B = 16.99%) :

$$\left(\frac{N}{S}\right)_{th} = 19.16\ 10^{-4}\,\Phi\,t\left(cm^{-2}\right) \tag{8}$$

and for the BN1 converter (d = 0.95 g cm^{-3}, mass fraction : B $\simeq$ 90%) :

$$\left(\frac{N}{S}\right)_{th} = 7.71\ 10^{-3}\,\Phi\,t\left(cm^{-2}\right) \tag{9}$$

The recorded track data were statistically analyzed. The mean track densities for the two converter materials and the respective experimental conditions are given in Table II.

The theoretical track densities were calculated using equations (8) and (9) for $Li_2B_4O_4(5H_2O)$ and BN1 converters respectively where the average neutron flux values are $1.5\ 10^6$ cm^{-2} s^{-1} for 100 kW reactor power and $1.5\ 10^{-4}$ cm^{-2} s^{-1} for 1 kW. From the comparison of the experimental and the theoretical track densities, one can see that the mean track densities over the canal section using different converters is in good accordance with the expected ones. This important result demonstrates the feasibility of neutron flux measurements in reactor facilities by means of SSNTD technique.

With help of equations (8) and (9), the tracks observed at different positions within the VC3 column were used to draw maps of neutron flux variations (Fig. 3, 4 and 5). Figure 3 was obtained using the $Li_2B_4O_4(5H_2O)$ conver-

TABLE II

Theoretical and experimental track densities for lithium tetraborate and BN1 converters and the respective irradiation conditions
Densités des traces théoriques et expérimentales pour les convertisseurs au tétraborate de lithium et au BN1 et conditions d'irradiation

Converter	Reactor power (kW)	Irradiation time (s)	Theoretical track density (cm^{-2})	Experimental track density (cm^{-2})
$Li_2B_4O_7(5H_2O)$	100	240	$4.59\ 10^5$	$4.61 \pm 1.83^*\ 10^5$
BN1 (E1)	1	3 600	$41.63\ 10^4$	$38.77 \pm 1.95\ 10^4$
BN1 (E2)	1	4 200	$48.57\ 10^4$	$48.19 \pm 1.35\ 10^4$

* The error in the last column represents the statistical uncertainty on the number of observed tracks (mean ± σ).

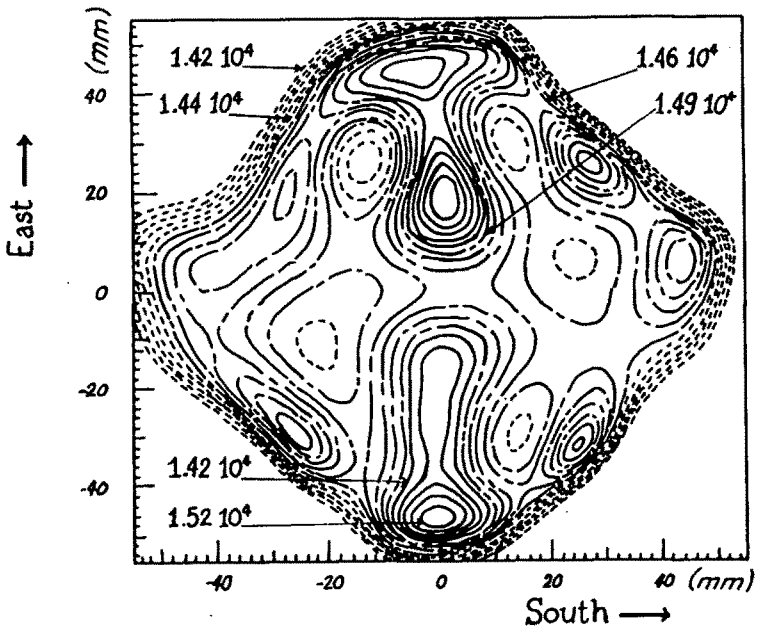

Fig. 3 – Neutron isoflux contours obtained with the lithium tetraborate converter at 100 kW reactor power. Dashed and dot-dashed contours are separated by 0.19 10^5 cm^{-2} s^{-1} and solid ones by 0.47 10^5 cm^{-2} s^{-1}. South and east are the geographical directions of the reactor.

Courbes d'isoflux de neutrons obtenues avec le convertisseur au tétraborate de lithium à 100 kW de puissance de fonctionnement du réacteur. Les courbes en tirets (- - - - et — - - —) sont séparées par 0,19 10^5 cm^{-2} s^{-1}, et les courbes en trait continus par 0,47 10^5 cm^{-2} s^{-1}. Sud et Est indiquent les régions géographiques du réacteur.

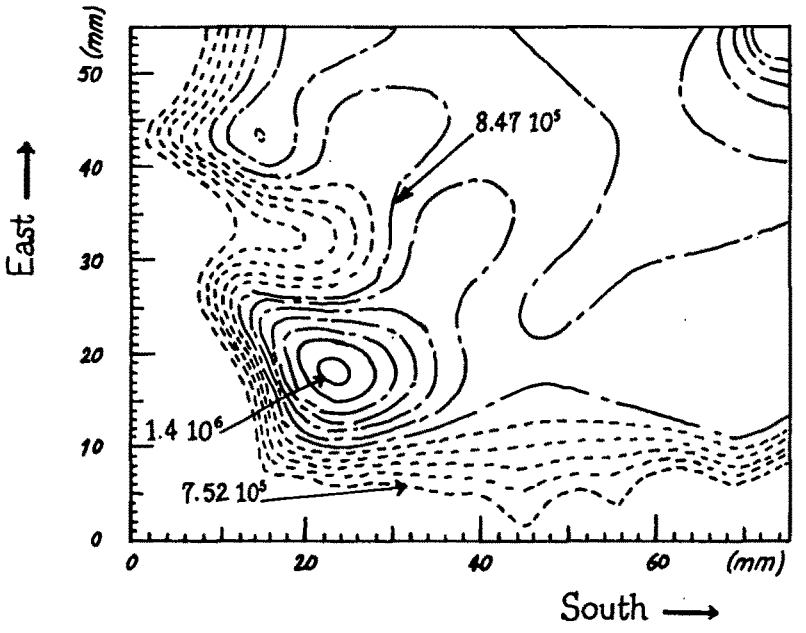

Fig. 4 – Neutron isoflux contours obtained with the BN1 converter at 1 kW reactor power, sheet E1. Dashed levels range from 1.32 10^4 cm^{-2} s^{-1} to 1.37 10^4 cm^{-2} s^{-1}, dot-dashed levels from 1.38 10^4 cm^{-2} s^{-1} to 1.41 10^4 cm^{-2} s^{-1} and solid contours from 1.42 10^4 cm^{-2} s^{-1} to 1.47 10^4 cm^{-2} s^{-1}.

Courbes d'isoflux de neutrons obtenues avec le convertisseur BN1 à 1 kW de puissance de fonctionnement du réacteur, feuille E1. Les courbes en pointillé couvrent la gamme allant de 1,32 10^4 cm^{-2} s^{-1} à 1,37 10^4 cm^{-2} s^{-1}, les courbes en traits discontinus varient de 1,38 10^4 cm^{-2} s^{-1} à 1,41 10^4 cm^{-2} s^{-1} et les courbes en traits continus montrent des variations allant de 1,42 10^4 cm^{-2} s^{-1} à 1,47 10^4 cm^{-2} s^{-1}.

ter. Dashed and dot-dashed isoflux contours are separated by 0.19 10^5 cm^{-2} s^{-1}, whereas solid contours near the position (24, 18) are separated by a value of 0.47 10^5 cm^{-2} s^{-1}. Neutron flux concentration can be easily observed at this region. This anomalous phenomenon may be caused by physical neutron flux gradient variations or non-uniformity of the lithium tetraborate layer on the CN85 film. In order to clarify this phenomenon, two experiments using BN1 converters were undertaken at the same irradiation position. The results obtained are shown in Figs. 4 and 5 for the E1 and E2 sheets respectively. Flux variations from the lowest to the highest levels are about 7% for E1 and 10% for E2. Both maps show that BN1 converter is more sensitive to neutron flux variations than lithium tetraborate. They also show that the layer of lithium tetraborate on the CN85 film is not uniform. Therefore the spatial variations of the neutron flux delivered by the VC3 were investigated using these two maps. The same small neutron flux concentration zones were observed in E1 and E2 in the same directions and positions of the column indicated by the coordinates (0,-46), (0,-16), (0,18), (0,44), (24,-30) and (32,24). This latter result shows the good reproducibility of neutrons flux variations when using BN1 converter.

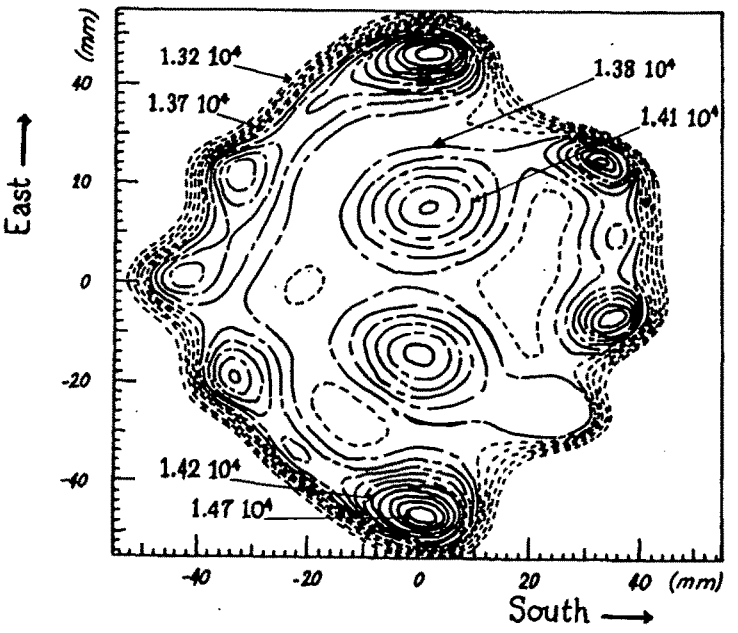

Fig. 5 – Neutron isoflux contours obtained with the BN1 converter at 1 kW reactor power, sheet E1. Dashed levels range from 1.42 10^4 cm^{-2} s^{-1} to 1.44 10^4 cm^{-2} s^{-1}, dot-dashed levels from 1.46 10^4 cm^{-2} s^{-1} to 1.49 10^4 cm^{-2} s^{-1} and solid contours from 1.50 10^4 cm^{-2} s^{-1} to 1.52 10^4 cm^{-2} s^{-1}.

Courbes d'isoflux de neutrons obtenues avec le convertisseur BN1 à 1 kW de puissance de fonctionnement du réacteur, feuille E2. Les courbes en pointillé couvrent la gamme allant de 1,42 10^4 cm^{-2} s^{-1} à 1,44 10^4 cm^{-2} s^{-1}, les courbes en traits discontinus varient de 1,46 10^4 cm^{-2} s^{-1} à 1,49 10^4 cm^{-2} s^{-1} et les courbes en traits continus montrent des variations allant de 1,50 10^4 cm^{-2} s^{-1} à 1,52 10^4 cm^{-2} s^{-1}.

These maps obtained using the BN1 converter show the uniformity of the thermal neutron flux over the upper end of the VC3 column. They thus give a direct image of the spatial distribution of the neutron flux where the concentration neutron flux zones can be clearly localized. Nevertheless, the neutron flux variations at this irradiation site still lay in an acceptable uncertainty for frequent irradiations (< 10%).

4. Conclusion

The detection technique proposed has advantageously been used to establish precise neutron flux cartographies and to mesure average neutron flux in a reactor facility. Among converter materials used to investigate thermal neutron flux spatial variation of large area of a neutron irradiation facility, the BN1 converter is found to be more sensitive to small variations than the lithium tetraborate one. ■

Remerciements

The authors wish to thank Mr A. Papé for his helpful remarks. We are also indebted to Mr R. Wohlgemuth, L. Schutz and the staff of the Strasbourg University nuclear reactor for their help during the irradiations.

REFERENCES

[1] BENTON E.V. – Application of nuclear track detectors in biology and medicine. *In* : Proceedings of the 11th Internationl conference on SSNTDs. (Fowler P.H., Clapham V.M., Eds). Oxford : Pergamon Press, 1981, 629-640.

[2] DUVAL Y., THELLIER M., HEURTEAUX C., WISSOCQ J.C. – Detection of stable isotopes with a (n, α) nuclear reaction : application to the measurement of unidirectional fluxes of borate in a plant. J. Radioanal. Chem., 1980, *55*, 297-306.

[3] EVANS R.D. – The atomic nucleus. New York : McGraw-Hill, 1955.

[4] INTERNATIONAL ATOMIC ENERGY AGENCY (IAEA). Neutron fluence measurements (Technical reports series N° 107), Vienna : IAEA, 1970.

[5] MARTINI F., HEURTEAUX C., WISSOCQ J.C., THELLIER M., STAMPFLER A. – Quantitative problems in using nuclear reactions and dielectric detectors for the detection of stable isotopes (^{6}Li and ^{10}B) in biological samples. J. Radioanal. Nucl. Chem., 1985, *91(1)*, 3-16.

[6] SEGHOUR A. – Dosimétrie et spectrométrie des neutrons. Recherche des conditions optimales pour le dosage du bore et application à la boroneutrothérapie. Thèse de Doctorat, Université Louis Pasteur de Strasbourg, N° 1644, Strasbourg 1993.

[7] TAKAGAKI M., MISHIMA Y. – Boron-10 quantitative analysis of neutron capture therapy on melanoma by spectrophotometric α-track reading. Nucl. Tracks Radiat. Meas., 1990, *17*, 531-535.

[8] THELLIER M., HENNEQUIN E., HEURTEAUX C., MARTINI F., PETTERSON M. – Quantitative estimations in neutron capture radiography. Nucl. Instrum. Methods, 1988, *B30*, 567-579.

[9] THURBER W.R., CARPENTER B.S. – (1979) Boron determination in silicon by nuclear track technique. J. Electrochem Soc., 1979, *125*, 654-657.